

# Structure of Quantum Chaotic Wavefunctions: Ergodicity, Localization, and Transport

L. Kaplan<sup>a\*</sup>

<sup>a</sup>Institute for Nuclear Theory and Department of Physics,  
University of Washington, Seattle, Washington 98195, USA

---

## Abstract

We discuss recent developments in the study of quantum wavefunctions and transport in classically ergodic systems. Surprisingly, short-time classical dynamics leaves permanent imprints on long-time and stationary quantum behavior, which are absent from the long-time classical motion. These imprints can lead to quantum behavior on single-wavelength or single-channel scales which are very different from random matrix theory expectations. Robust and quantitative predictions are obtained using semiclassical methods. Applications to wavefunction intensity statistics and to resonances in open systems are discussed.

*PACS:* 05.45.+b, 03.65.Sq

*Keywords:* wave function statistics, quantum transport, quantum ergodicity.

---

## 1. Introduction

The structure of quantum wavefunctions and the closely related problem of quantum transport in classically non-integrable systems have received much attention recently from a variety of physics communities. Questions concerning the quantum behavior of systems with a generic classical limit are of course of great fundamental interest; they are also very relevant not only for nanostructure and mesoscopics experiments [1], but also for understanding phenomena in areas as diverse as atomic physics [2], molecular and chemical physics [3], microwave physics [4], nuclear physics [5], and optics [6]. Combined with knowledge about spectral properties, wavefunction information can be used to address conductance curves, susceptibilities, resonance statistics, and delay times in ballistic quantum dots. Similar wavefunction and transport issues arise in other fields, in the study of resonance statistics in microwave cavities, photoionization cross sections, chemical reaction rates, spectra of Rydberg

atoms, lifetimes and emission intensities for resonant optical cavities, and  $S$ -matrix properties in many systems.

In the classically integrable case, quantum wavefunctions are known to be associated with the invariant tori of the corresponding classical dynamics, satisfying the Einstein–Brillouin–Keller (EBK) quantization conditions [7]. Classical–quantum correspondence in the ergodic case is, however, more subtle. Here, the typical classical trajectory uniformly visits all of the energetically available phase space, so naively the typical quantum wavefunction should also have uniform amplitude over an entire energy hypersurface, up to the inevitable (Gaussian random) fluctuations. Such behavior follows directly from Random Matrix Theory (RMT), which has been proposed by Bohigas, Giannoni, and Schmit [8] to be the proper description of quantum chaotic behavior in the semiclassical limit (i.e. in the limit where the de Broglie wavelength  $\lambda$  becomes small compared to the system size). A similar conjecture by Berry [9] states that a typical quantum wavefunction in

---

\*lkaplan@phys.washington.edu

this same limit should look locally like a random superposition of plane waves of fixed energy, with momenta pointing in all possible directions.

RMT [10], a natural quantum analogue of classical ergodicity, turns out to describe well *spectral properties on small energy scales* (e.g. the distribution of nearest neighbor level spacings in the spectrum), but does not always provide a valid description of *wavefunction structure and transport* properties. Scars [11] provide one of the most visually striking examples of strong deviation from RMT wavefunction behavior; other examples include slow ergodic systems [12] and Sinai-type systems [13]. In all these cases, non-RMT behavior can be quantified, semiclassically predicted, and observed.

Section 2 addresses the problem of wavefunction ergodicity in broad terms. We are interested both in general questions concerning the implications of global classical properties (such as ergodicity or mixing) on quantum behavior and also in the way in which specific classical structures (such as unstable periodic orbits) may leave their imprints on the quantum eigenstates. Several examples, including that of Sinai-type systems, are discussed in Section 2.3. Sections 3 and 4 focus on the scar phenomenon and quantitative predictions. The overview format of this presentation requires us to omit most derivations; references to more detailed discussions in the literature can be found throughout.

## 2. Ergodic wavefunction structure and quantum transport

### 2.1. Coarse-grained vs. microscopic ergodicity

We must distinguish between two ways of extending classical notions of ergodicity to the quantum case [12]. First, we may consider wavefunction intensity integrated over a classically defined region  $\mathcal{R}$ , in the regime where the wavelength  $\lambda$  becomes small compared to the size of  $\mathcal{R}$ . As can be shown rigorously [14], in this limit the integrated intensity approaches a constant (equal to the area of  $\mathcal{R}$  as a fraction of total phase space) for almost all wavefunctions. The result requires only long-time classical ergodicity and

quantum-classical correspondence at short times; a half-page physicists' derivation can be found in [15]. We note that this macroscopic or "coarse-grained" type of quantum ergodicity is clearly implied by RMT, but is in fact a much weaker condition. Quantum wavefunction structure on coarse-grained scales is relevant for studying conductance and conductance fluctuations through wide, multichannel leads, for fast decay processes, and generally for analyzing open systems in the overlapping resonance regime.

RMT, on the other hand, is a prediction about wavefunction uniformity at the quantum scale, i.e. on the scale of a single wavelength (or single momentum channel, or most generally at the scale of a single  $\hbar$ -sized cell in phase space). This kind of uniformity is a much stronger condition than coarse-grained ergodicity, and several examples will be given later in this section where microscopic quantum ergodicity is violated in classically ergodic systems. Wavefunction structure at the quantum scale is relevant, obviously, for transport through narrow (or tunneling) leads.

### 2.2. Measures of microscopic ergodicity

First we must define quantitative measures of ergodicity or localization at the microscopic scale [12]. Let  $|n\rangle$  be an  $N$ -dimensional basis of eigenstates, and  $|a\rangle$  some localized test basis, e.g. position, momentum, or phase space Gaussians, as is physically appropriate in a given system. For example, in discussing Anderson-type lattice localization, we may choose our test basis  $|a\rangle$  to be the position basis, whereas in scattering problems plane waves may be a more natural choice. Sometimes we take  $|a\rangle$  to be the eigenstates of a zeroth-order Hamiltonian  $H_0$  or of a zeroth-order scattering matrix  $S_0$ . We are then interested in the wavefunction intensities  $P_{an} = |\langle a|n\rangle|^2$  and their correlations. For simplicity of presentation we assume there are no conserved quantities, so classically nothing prevents each eigenstate  $|n\rangle$  for overlapping equally with each  $|a\rangle$  (of course, the formalism generalizes naturally to the more general case of classical symmetries, see [16]). We adopt the normalization convention

$$\langle P_{an} \rangle = 1, \quad (1)$$

where the averaging is done over test states  $|a\rangle$ , over wavefunctions  $|n\rangle$ , or over an appropriate ensemble of systems.

The first nontrivial moment of the  $P_{an}$  distribution is the *inverse participation ratio*:

$$\text{IPR}_a = \frac{1}{N} \sum_{n=1}^N P_{an}^2 \geq 1, \quad (2)$$

which measures the mean squared wavefunction intensity at  $|a\rangle$ , or, alternatively, the inverse fraction of wavefunctions having significant intensity at  $|a\rangle$ .  $\text{IPR}_n$ , the mean squared intensity of a single wavefunction  $|n\rangle$  averaged over position  $|a\rangle$ , is defined analogously: it measures the inverse fraction of phase space covered by  $|n\rangle$ . A global IPR measure may also be conveniently defined:

$$\text{IPR} = \frac{1}{N} \sum_{a=1}^N \text{IPR}_a = \frac{1}{N} \sum_{n=1}^N \text{IPR}_n \geq 1, \quad (3)$$

and provides a simple one-number measure of the degree of localization in a quantum system. An IPR of unity corresponds to perfect ergodicity (each wavefunction having equal overlaps with all test states), while  $\text{IPR} = N$  indicates the greatest possible degree of localization (the wavefunctions  $|n\rangle$  being identical with the test states  $|a\rangle$ ).

Besides being the first nontrivial moment of the intensity distribution, the IPR measure is useful because of its connection with dynamics. For example,  $\text{IPR}_a$  is proportional to the averaged long-time return probability for a particle launched initially in state  $|a\rangle$ :

$$\text{IPR}_a = N \lim_{T \rightarrow \infty} \frac{1}{T} \sum_{t=0}^{T-1} |\langle a | e^{-i\hat{H}t/\hbar} | a \rangle|^2. \quad (4)$$

It is intuitively clear that enhanced long-time return probability is associated with increased localization. We may generalize  $\text{IPR}_a$  to a transport or wavefunction correlation measure between local states  $|a\rangle$  and  $|b\rangle$ :

$$P_{ab} = \sum_{n=1}^N \frac{P_{an}P_{bn}}{N} = \lim_{T \rightarrow \infty} \frac{N}{T} \sum_{t=0}^{T-1} |\langle a | e^{-i\hat{H}t/\hbar} | b \rangle|^2. \quad (5)$$

Of course, the mean  $\frac{1}{N} \sum_b P_{ab} = 1$  by unitarity; the simplest nontrivial measure of transport effi-

ciency is thus

$$Q_a = \frac{1}{N} \sum_b P_{ab}^2 \geq 1, \quad (6)$$

which measures the inverse of the fraction of phase space accessible from  $|a\rangle$  at long times.  $Q_a = 1$  for all  $|a\rangle$  (the RMT result for  $N \rightarrow \infty$ ) indicates perfect long-time transport, and vanishing wavefunction correlations.

### 2.3. Examples

The Random Matrix Theory description is free of all dynamical information about the system under study and thus can hardly be expected to provide a correct statistical description of all quantum behavior. It serves, however, as a very useful baseline with which real quantum chaotic behavior may be compared. In RMT, the wavefunction intensities  $P_{an}$  are squares of Gaussian random variables and so are drawn from a  $\chi^2$  distribution (of one degree of freedom for real overlaps  $\langle a|n\rangle$  or two for complex overlaps), with a mean value of unity. This easily leads to  $\text{IPR}_{\text{RMT}} = 3$  in the real case or 2 in the complex case. Notice that even in RMT, quantum fluctuations cause wavefunctions to be less ergodic than the classical expectation  $\text{IPR}_{\text{Clas}} = 1$ . By quantum localization, however, we always mean fluctuation in the intensities *in excess of what would be expected from a Gaussian random model*, i.e.  $\text{IPR} > \text{IPR}_{\text{RMT}}$ . Examples abound of such anomalous quantum behavior in classically ergodic systems, and several are described below. We also mention here that in RMT, the channel-to-channel transport efficiency  $P_{ab}$  approaches unity for all channels  $|a\rangle$ ,  $|b\rangle$  in the  $N \rightarrow \infty$  semiclassical limit.

(i) *Scarring* is the anomalous enhancement or suppression of quantum wavefunction intensity on the *unstable* periodic orbits of the corresponding classical system. This localization behavior is perhaps surprising from a naive classical point of view, since in the time domain (see Eq. 4) it implies an enhanced long-time return probability for a wavepacket launched on an unstable periodic orbit. Paradoxically, this is in contrast with the classical behavior, where a probability distribution spreads itself evenly over the entire ergodic space at long times and retains no memory

of its initial state. Quantum long-time dynamics, which of course contains phase information, thus retains a much *better* memory of the short-time classical behavior than does the long-time classical dynamics, for arbitrarily small values of  $\hbar$ . Specifically, for a wavepacket  $|a\rangle$  optimally oriented on an orbit of instability exponent  $\beta$ , we have [11]

$$\text{IPR}_{\text{Scar}} = \left[ \sum_{m=-\infty}^{\infty} \frac{1}{\cosh \beta m} \right] \text{IPR}_{\text{RMT}} \quad (7)$$

$$\rightarrow \frac{\pi}{\beta} \text{IPR}_{\text{RMT}} \gg \text{IPR}_{\text{RMT}}, \quad (8)$$

where the limiting form is valid for weakly unstable orbits ( $\beta \ll 1$ ). A finite fraction of order  $\beta$  of all wavefunctions are *scarred*: they have intensity  $O(\beta^{-1})$  on the periodic orbit compared with the mean intensity, while most of the remaining wavefunctions are *antiscarred*, and have intensities on the orbit as small as  $\exp(-\pi^2/2\beta)$  compared with the mean. The source of this localization effect will be outlined in Section 3. The transport measure  $P_{ab}$  is also affected by scarring: if both leads  $|a\rangle$  and  $|b\rangle$  are located near periodic orbits,  $P_{ab}$  can be enhanced or suppressed depending on whether the two orbits are “in-phase” or “out-of-phase” in the range of energies considered. These long-time transport results are  $\hbar$ -independent and are obtained directly from the short-time linearized classical dynamics.

(ii) *The tilted wall billiard* (a rectangular box with one wall tilted relative to the other three), is a classically ergodic system in which the wavefunctions (as measured by the IPR) become *less and less ergodic* in the classical  $\hbar \rightarrow 0$  (or  $\lambda \rightarrow 0$ ) limit [12]. (This kind of behavior is possible because the  $\hbar \rightarrow 0$  limit fails to commute with the infinite time  $t \rightarrow \infty$  limit.) Specifically, for wavefunctions expressed in channel (momentum) space, we have

$$\text{IPR}_{\text{Tilted}} \sim \lambda^{-1/2} / \log \lambda^{-1} \rightarrow \infty. \quad (9)$$

This anomalous wavefunction behavior at the single-channel scale is entirely consistent with ergodicity on coarse-grained scales; coarse-graining over  $\sim \lambda^{-1} / \log \lambda^{-1}$  channels is required to retrieve the classical behavior. Quantum transport

in these systems is also anomalous and is dominated by diffractive effects (due to the slowness of classical phase space exploration).

(iii) As a final example we mention *the Sinai billiard*, a paradigm of classical chaos [17]. This consists of a circular obstruction of diameter  $d \gg \lambda$  placed inside a rectangle. Again using momentum channels for the test basis  $|a\rangle$ , we obtain [13]

$$\text{IPR}_{\text{Sinai}} \sim (\log \lambda^{-1}) / d \rightarrow \infty \quad (10)$$

for fixed  $d$  in the  $\lambda \rightarrow 0$  limit. Again, we see nonergodic  $\lambda \rightarrow 0$  wavefunctions in a classically ergodic system. The distributions of wavefunction intensities  $P_{an}$  and IPR’s ( $\text{IPR}_a$  and  $\text{IPR}_n$ , see Eq. 2) all display power-law tails (in contrast with the exponential tail prediction of RMT). Transport is similarly anomalous: for the typical channel  $|a\rangle$ ,  $Q_a \sim d^{-1}$  (see Eq. 6); i.e. at long times a given channel is coupled to only a fraction  $\sim d \ll 1$  of all other channels.

### 3. Scars of quantum chaotic wavefunctions

#### 3.1. Phenomenology and conceptual issues

Scars have been observed experimentally and numerically in a wide variety of systems. These include semiconductor heterostructures, where scars are observed to affect tunneling rates from a 2D electron gas into a quantum well [18], microwave cavities [19], the hydrogen atom in a uniform magnetic field [20], acoustic radiation from membranes [21], and the stadium billiard, for which wavefunctions as high as the millionth state in the spectrum can be numerically analyzed [22]. Nevertheless, confusion over the definition and measures of scars (and the dearth of quantitative predictions) have until recently led some to question the existence of a scar theory, and even to doubt the survival of the phenomenon in the classical limit. Recent theoretical developments [11] enable us to make robust, quantitative predictions about how strongly a given orbit will be scarred and how often, as a function of energy and other system parameters; real comparison with numerical and experimental data is therefore made possible. We also note that statistical and quantitative data, rather than anecdotal (in the form of wavefunction plots) is necessary as

a test of scar theory or of any other theory of a localization phenomenon, since considerable fluctuations of wavefunction intensity occur even in the context of RMT (see discussion in first paragraph of Section 2.3).

We address some common misconceptions and summarize key facts about the scar phenomenon: (i) Scarring is associated with *unstable* periodic orbits, not with stable or marginally stable ones, though these of course also do attract wavefunction intensity; a qualitative difference arises because of classical–quantum noncorrespondence in the unstable case (Section 2.3(i)). (ii) Weak scars are not always visible to the naked eye; scars are defined and measured according to a statistical definition. (iii) Scarring predictions are robust, valid even when the exact dynamics is not known well enough to allow individual eigenstates to be determined either quantum mechanically or semi-classically. (iv) The amount of scarring associated with individual eigenfunctions varies significantly from state to state, but in accordance with a theoretically predicted distribution. (v) If an optimally chosen phase space basis is used, the typical intensity enhancement factor as well as the full distribution of scar intensities can be given as a function of the instability exponent  $\beta$ .

### 3.2. Short-time effects on stationary properties

We define the autocorrelation function for test state  $|a\rangle$ :

$$A(t) = \langle a | \exp[-iHt] | a \rangle, \quad (11)$$

the Fourier transform of which is the local density of states (LDOS)

$$S(E) = \sum_n P_{an} \delta(E - E_n). \quad (12)$$

Then, if we know the statistical properties of the return amplitude  $A(t)$ , we also know the statistical properties of the LDOS at  $|a\rangle$ , and specifically of the wavefunction intensities  $P_{an}$  (see e.g. Eq. 4). Furthermore, given information about the return amplitude  $A(t)$  for short times only (say for  $|t| < T_0$ ), we immediately obtain the LDOS envelope  $S_{\text{smooth}}(E)$ , which is the energy-smoothed (on scale  $\hbar/T_0$ ) version of the true line-

spectrum  $S(E)$ . So large short-time recurrences in  $A(t)$  get ‘burned into’ the spectrum.

Specifically, if  $|a\rangle$  is a minimum uncertainty wavepacket optimally placed on a periodic orbit of period  $P$ , then at integer multiples  $t = mP$  of this period, by Gaussian integration we easily obtain [11]

$$A_{\text{short}}(t) = \exp[imS/\hbar] / \sqrt{\cosh \beta m}, \quad (13)$$

where the classical orbit has action  $S$  and instability exponent  $\beta$ . For small  $\beta$ , the Fourier transformed spectral envelope  $S_{\text{smooth}}(E)$  has bumps of width scaling as  $\beta/P$  and height scaling as  $\beta^{-1}$ . Now after the mixing time ( $\sim \beta^{-1} \log N$ ), escaping probability starts returning to the origin, leading to fluctuations in the spectral envelopes, and eventually to discrete delta-function peaks (Eq. 12). The nonlinear scar theory allows the long-time returning amplitude to be analyzed as a homoclinic orbit sum [11], and leads to the prediction that the spectral intensities are given by  $\chi^2$  variables multiplying the short-time envelope:

$$P_{an} = |r_{an}|^2 S_{\text{smooth}}(E_n), \quad (14)$$

where the  $r_{an}$  follow a Gaussian random distribution of variance unity.

## 4. Quantitative predictions for scar effects

### 4.1. Wavefunction intensity statistics

As a simple application, we may compute the distribution of wavefunction intensities on a periodic orbit of instability exponent  $\beta$  [23]. For complex wavefunctions, the probability to have an intensity exceeding the mean by a factor  $x$  is given by  $\exp(-x)$  in RMT; on a periodic orbit the tail of the distribution is instead given by

$$P(\beta, x) = C \beta (\beta x)^{-1/2} e^{-\beta x/Q}, \quad (15)$$

where  $C$  and  $Q$  are known numerical constants. Similarly, the tail of the overall intensity distribution (sampled over the entire phase space) is given by

$$P(\beta, x) = C' \beta \hbar (\beta x)^{-3/2} e^{-\beta x/Q}, \quad (16)$$

where  $\beta$  is now the exponent of the least unstable periodic orbit. These two results are illustrated

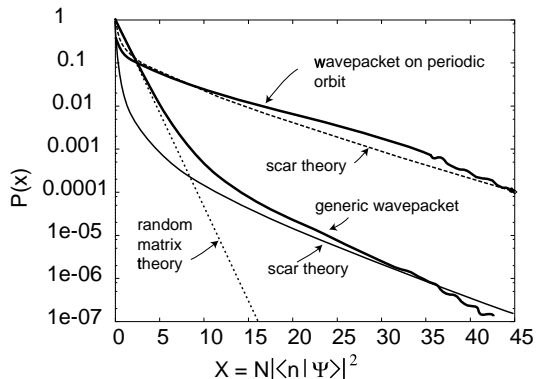


Figure 1. Cumulative wavefunction intensity distribution (a) as measured by a Gaussian test state optimally centered on a periodic orbit with instability exponent  $\beta = \log 2$ , plotted as the upper thick curve with scar theory prediction for the tail (Eq. 15) given by dashed curve, and (b) averaged over the entire phase space of size  $200h$ , plotted as lower thick curve with theory for the tail (Eq. 16) given by solid curve. The dotted line is the RMT exponential prediction (after [23]).

in Fig. 1. Finally, for an ensemble of systems, a power-law tail is obtained, in contrast with the exponential prediction of RMT, and large intensities have been observed numerically with frequency exceeding by  $\sim 10^{30}$  the RMT predictions.

#### 4.2. Enhancement in probability to remain

The above methods can also be applied to the open systems case [24]. Consider the probability to remain inside a chaotic quantum well coupled to the outside via a tunneling lead. For a lead optimally placed with respect to a periodic orbit of exponent  $\beta \ll 1$ , the long-time probability to remain is enhanced by a factor  $\exp(\pi^2/2\beta)$  (see Fig. 2), compared with the RMT expectation. (The enhancement is due the antiscarred states (Section 2.3(i)), which have very small coupling to the lead.) Of course, the classical probability to remain is exponential and independent of lead position for a chaotic system with a narrow lead. So once again we see long-time quantum mechanics retaining an imprint of short-time classical structures which is absent from long-time classical be-

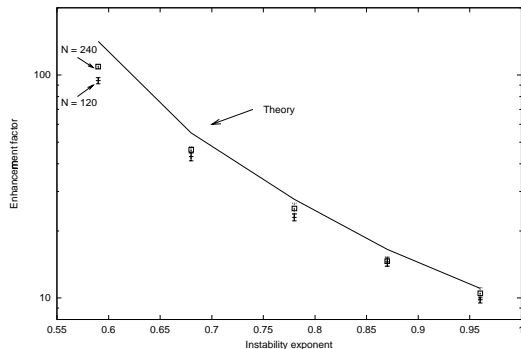


Figure 2. The long-time enhancement of the probability to remain in a weakly open system when the tunneling lead is placed on a periodic orbit is plotted as a function of the instability exponent  $\beta$  of the orbit. Data is shown for system sizes  $N = 120$  (plusses) and  $N = 240$  (squares). The  $N \rightarrow \infty$  theoretical prediction (Section 4.2), growing exponentially with decreasing  $\beta$ , is shown as a solid curve. For large  $\beta$ , the enhancement factor converges to 1, the RMT prediction (after [24]).

havior. The analysis can of course be extended to the study of conductance peak statistics in two lead systems, where one or both leads are located near short periodic orbits (compare with the discussion of  $P_{ab}$  statistics in Section 2.3(i)).

## 5. Conclusions

We have seen that wavefunction structure and transport in classically ergodic systems, including the paradigmatic Sinai billiard system, can differ greatly from RMT expectations, and in fact can deviate further and further from RMT in the semiclassical limit. This non-ergodic quantum behavior at the scale of single wavelengths or single quantum channels can be quantitatively and robustly predicted using only short-time classical information. This anomalous small-scale quantum behavior is also entirely consistent with ergodicity on coarse-grained scales, as studied by Schnirelman, Zelditch, and Colin de Verdiere.

Scarring is a fascinating example of the influ-

ence of identifiable classical structures on stationary quantum properties (e.g. eigenstates) and long-time quantum transport in classically chaotic systems. Short unstable periodic orbits leave a strong imprint on the long-time properties of the quantum chaotic system, even though classical dynamics loses all memory of these structures at long times. Scar theory makes robust and quantitatively verified predictions about properties such as the wavefunction intensity distribution in a chaotic system, including the power-law tail observed after ensemble averaging. A lead centered on an unstable periodic orbit has been shown to produce many exponentially narrow quantum resonances, even though the decay times are very long compared with all other time scales in the problem. Enhancement factors of 10 to 100 in the total probability to remain are easily observed for moderate values (1.0 to 0.5) of the instability exponent.

## 6. Acknowledgments

It is a pleasure to thank E. J. Heller for many fruitful discussions. This work was supported by the National Science Foundation under Grant No. 66-701-7557-2-30.

## REFERENCES

1. Y. Alhassid and H. Attias, *Phys. Rev. Lett.* **76**, 1711 (1996); E. E. Narimanov, N. R. Cerutti, H. U. Baranger, and S. Tomsovic, cond-mat/9812165.
2. A. F. Brunello, T. Uzer, and D. Farrelly, *Phys. Rev. Lett.* **76**, 2874 (1996); J. Main and G. Wunner, *J. Phys.* **B 27**, 2835 (1994); G. Benenti, G. Casati, and D. L. Shepelyansky, *Phys. Rev. A* **56**, 3297 (1997).
3. N. Hashimoto and K. Takatsuka, *J. Chem. Phys.* **108**, 1893 (1998); F. J. Arranz, F. Borondo, and R. M. Benito, *Eur. Phys. Journal D* **4**, 181 (1998).
4. U. Dorr, H.-J. Stockmann, M. Barth, and U. Kuhl, *Phys. Rev. Lett.* **80**, 1030 (1998); S. Sridhar and E. J. Heller, *Phys. Rev. A* **46**, R1728 (1992).
5. V. Zelevinsky, B. A. Brown, N. Frazier, and M. Horoi, *Phys. Rep.* **276**, 85 (1996); B. Laurantzen, P. F. Bortignon, R. A. Broglia, and V. G. Zelevinsky, *Phys. Rev. Lett.* **74**, 5190 (1995).
6. J. U. Nockel and A. D. Stone, *Nature* **385**, 45 (1997).
7. M. V. Berry and M. Tabor, *Proc. Roy. Soc. A* **349**, 101 (1976); M. V. Berry and M. Tabor, *J. Phys. A* **10**, 371 (1977).
8. O. Bohigas, M.-J. Giannoni, and C. Schmit, *J. Physique Lett.* **45**, L-1015 (1984).
9. M. V. Berry, in *Chaotic Behaviour of Deterministic Systems*, ed. by G. Iooss, R. Helleman, and R. Stora (North-Holland 1983) p. 171.
10. M. L. Mehta, *Random Matrices*, Academic Press (1991); T. A. Brody, J. Flores, J. B. French, P. A. Mello, A. Pandey, and S. S. M. Wong, *Rev. Mod. Phys.* **53**, 385 (1981).
11. E. J. Heller, *Phys. Rev. Lett.* **53**, 1515 (1984); L. Kaplan, *Nonlinearity* **12**, R1 (1999).
12. L. Kaplan and E. J. Heller, *Physica D* **121**, 1 (1998).
13. L. Kaplan and E. J. Heller, "Short Time Effects on Eigenstate Structure in Sinai Billiards and Related Systems," in preparation.
14. A. I. Schnirelman, *Usp. Mat. Nauk.* **29**, 181 (1974); Y. Colin de Verdiere, *Commun. Math. Phys.* **102**, 497 (1985); S. Zelditch, *Duke Math. J.* **55**, 919 (1987).
15. L. Kaplan, "Quantization Ambiguity, Ergodicity, and Semiclassics," quant-ph/9906065.
16. E. B. Stechel and E. J. Heller, *Ann. Rev. Phys. Chem.* **35**, 563 (1984); E. J. Heller, *Phys. Rev. A* **35**, 1360 (1987).
17. Ya. G. Sinai, *Funct. Anal. Appl.* **2**, 61 and 245 (1968); *Russ. Math. Surv.* **25**, 137 (1970).
18. T. M. Fromhold et al., *Phys. Rev. Lett.* **75**, 1142 (1995); P. B. Wilkinson et al., *Nature* **380**, 608 (1996).
19. S. Sridhar, *Phys. Rev. Lett.* **67**, 785 (1991); S. Sridhar, D. O. Hogenboom, and B. A. Willemsen, *J. Stat. Phys.* **68**, 239 (1992); J. Stein and H.-J. Stockman, *Phys. Rev. Lett.* **68**, 2867 (1992).
20. D. Wintgen and A. Honig, *Phys. Rev. Lett.* **63**, 1467 (1989); K. Muller and D. Wintgen, *J. Phys. B* **27**, 2693 (1994).

21. D. Delande and D. Sornette, *J. Acoust. Soc. America* **101**, 1793 (1997).
22. B. Li, *Phys. Rev. E* **55**, 5376 (1997); B. Li and B. Hu, *J. Phys. A* **31**, 483 (1998).
23. L. Kaplan, *Phys. Rev. Lett.* **80**, 2582 (1998).
24. L. Kaplan, *Phys. Rev. E* **59**, 5325 (1999).